P H Y S I C A L   R E V I E W   L E T T E R S

Energetic Surface Smoothing of Complex Metal-Oxide Thin Films

P. R. Willmott,* R. Herger, C. M. Schlepütz, D. Martoccia, and B. D. Patterson

Swiss Light Source, Paul Scherrer Institut, CH-5232 Villigen, Switzerland
(Received 19 January 2006; published 2 May 2006)

A novel energetic smoothing mechanism in the growth of complex metal-oxide thin films is reported from *in situ* kinetic studies of pulsed laser deposition of $La_{1-x}Sr_xMnO_3$ on $SrTiO_3$, using x-ray reflectivity. Below 50% monolayer coverage, prompt insertion of energetic impinging species into small-diameter islands causes them to break up to form daughter islands. This smoothing mechanism therefore inhibits the formation of large-diameter 2D islands and the seeding of 3D growth. Above 50% coverage, islands begin to coalesce and their breakup is thereby suppressed. The energy of the incident flux is instead rechanneled into enhanced surface diffusion, which leads to an increase in the effective surface temperature of $\Delta T \approx 500$ K. These results have important implications on optimal conditions for nanoscale device fabrication using these materials.

One of the primary goals of modern condensed-matter physics is to facilitate the use in solid-state devices of novel materials, such as the diverse family of strongly correlated electron systems [1]. Their chemical and crystallographic complexity, however, presents a formidable challenge regarding the control of morphology and crystalline quality during film growth. In this respect, nonthermal growth techniques such as pulsed laser deposition (PLD) and sputtering have proved to be among the most promising to date [2,3]—the energetic particle beams used in these methods interact with the growing surface in ways that are unavailable to thermal deposition techniques [4–6]. This can lead to unusual and often advantageous growth kinetics and can force a film to grow under conditions far from thermal equilibrium [7–10]. A deeper understanding of the underlying atomistic processes is thus important for optimizing growth conditions to obtain nanoscale structures of high-quality material.

Because of its nonthermal nature, PLD is one of only a handful of techniques that is able to transfer chemically complex material congruently from the bulk to thin film [2]. In addition, the pulsed flux (of the order of 10^{20} atoms $cm^{-2}\,s^{-1}$) and associated supersaturation above the surface promotes the initial dense nucleation of small two-dimensional islands. These can be as small as a single atom and help promote two-dimensional film growth [3,11]. Before a monolayer (ML) is completed, however, conventional (i.e., thermal) growth models predict that the next monolayer(s) will begin to seed far away from step edges on large 2D islands, leading eventually to 3D growth [11]. How soon this happens depends on the effective surface diffusion constants (a) between the islands in the growing layer, leading to 2D island ripening, and (b) on top of the islands, resulting in interlayer mass transport [12]. This simple treatment is unable to explain the many reports in the literature in which thin films consisting of several hundred ML continue to grow two dimensionally, because it ignores processes involving the redistribution of the kinetic energy of the incoming flux as

it impinges on the surface layer. It is these processes which need to be better understood.

Several theoretical studies have addressed this issue [4,5,13]. Particularly relevant is the work presented by Jacobsen *et al.*, in which the nonthermal interaction of an energetic incident atom with the surface (which occurs on the ps time scale) and thermal diffusion processes on the time scale of seconds were described by molecular dynamics (MD) simulations and kinetic Monte Carlo simulations, respectively, in a single model [14,15]. These studies of homoepitaxy of transition metals indicated that, as well as enhancing surface diffusion, particles impinging with kinetic energies of tens to hundreds of eV promoted smooth growth by inserting themselves into surface islands, provided they land near the descending edge of an island or terrace.

In this Letter, we report on a possible mechanism for promoting 2D growth in complex metal-oxide thin films, involving impact-induced island breakup, during PLD of the perovskite $La_{1-x}Sr_xMnO_3$ (LSMO) grown heteroepitaxially on $SrTiO_3$ (STO).

Experiments were performed at the Surface Diffraction station of the Materials Science beam line at the Swiss Light Source [16]. The *in situ* PLD setup and evidence for the high crystalline quality of the films have been described elsewhere [17,18]. Films of LSMO were grown on TiO_2-terminated STO(001) by ablating a dual $LaMnO_3/SrMnO_3$ target rod. In this study, $x = 0.34$ (checked by Rutherford backscattering spectroscopy). Film growth was monitored by recording the x-ray reflectivity at the $(0\ 0\ \frac{1}{2})$ point of the specular crystal truncation rod (CTR). This signal oscillates during 2D island coalescence growth, due to (a) repeated roughening and smoothing, with a periodicity of 1 ML, and (b) interference between reflections from the film surface and the film-substrate interface (i.e., Kiessig fringes), with a periodicity of 2 ML.

Two deposition modes were employed. The first was "conventional" PLD growth at 10 Hz using a fixed repetition-rate Nd:YAG laser ($\lambda = 266$ nm). The 1 Hz

PHYSICAL REVIEW LETTERS

frame rate of the pixel area x-ray detector employed for these studies therefore precluded the resolution of any thermal relaxation in between laser shots. To observe thermal kinetic effects, an interrupted mode was also used, in which short bursts of ablation (here, 12 laser shots, the minimum needed to ensure that the composition x of the film remained constant [17]) were separated from one another by intervals of a few tens of seconds of no deposition, during which changes in the specular intensity due to thermal relaxation could be monitored. This interrupted PLD is similar to pulsed laser *interval* deposition described by Rijnders *et al.*, [8], the difference being that here only small fractions of a ML are deposited with each burst.

Growth oscillations during conventional PLD are shown in Fig. 1. Two-dimensional growth persists up to several tens of nm film thickness. Reflectivity curves of films over 100 nm thick show clear Kiessig fringes and can be fit to a roughness of well under 1 ML [17]. Surface smoothing therefore appears to be sufficiently rapid that little or no buildup occurs on top of each growing ML within the 20 s required for completion.

An example of growth using interrupted PLD is shown in Fig. 2 for deposition of the third ML. A description of the changes in the surface step density due to thermal surface diffusion has been proposed by Stoyanov and Michailov [12] and adapted to transient reflection high-energy electron-diffraction signals in PLD by Rijnders [19], although the model does not take into account changes in surface morphology due to energetic effects. Two constants τ_1 and τ_2 describe, respectively, the characteristic time to reach a step edge within the unfilled parts of the growing ML and that to cross the top of the islands making up the incomplete ML and drop into the growing layer. τ_1 dominates at low coverage θ, while τ_2 governs at higher coverages. For reasons that will become clear, it was difficult using the present temporal resolution to obtain reliable fits for τ_1, and we concentrate here on the second half of ML coverage, dictated by τ_2. In a first approximation, by ignoring τ_1, τ_2 can be fit by the expression [19]

$$I = I_0 + \Delta I\{1 - \exp[-(t - t_0)/\tau_2]\}, \quad (1)$$

whereby I_0 and t_0 are the intensity and time immediately after the 12-shot ablation burst, respectively, ΔI is the change in the specular reflection after complete thermal relaxation, and τ_2 is given by

$$\tau_2 = \frac{\theta}{D_S(\mu_l^{(0)})^2 \pi N_S}. \quad (2)$$

Here, $\mu_l^{(0)} = 2.40$ is the first root of the zeroth order Bessel function, N_S is the nucleation density, and D_S is the surface diffusion coefficient given by $D_S = D_0 \exp(-E_a/kT)$, where E_a is the surface diffusion barrier. Note that in this model, τ_2 is directly proportional to θ and should increase linearly from the start of the ML coverage.

The data for the second half of the ML growth have been fit using two free parameters ΔI and τ_2, and I_0 and t_0, which were allowed to deviate from their starting estimates only over ± 250 arbitrary intensity units and ± 1 s, respectively. The fits and the change in τ_2 with ML coverage θ are shown in the inset of Fig. 2. The thermal relaxation times are several tens of seconds for the second half of monolayer coverage, i.e., significantly longer than the time to grow a single ML when using conventional PLD. This difference demonstrates the beneficial influence of the impinging flux on the evolution and kinetics of the incomplete monolayer, which we will address more quantitatively below.

The high degree of supersaturation of the impinging flux of particles in PLD results in a high density of stable nucleation sites, each of the order of 1 to 2 atoms in size [3]. MD calculations predict an enhanced surface diffusion length of the order of 10 atomic spacings in the first few picoseconds after the particle lands on the surface [20]. The first pulse of impinging particles nucleates unit-cell or
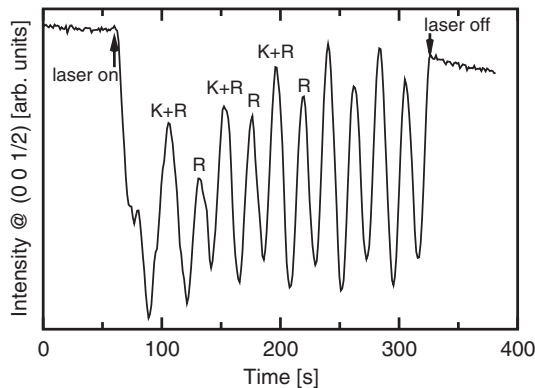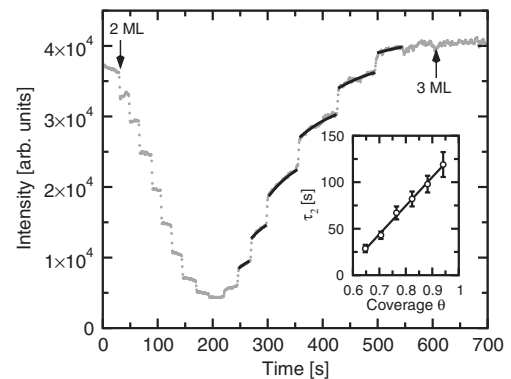

FIG. 1. Growth oscillations during conventional PLD of LSMO on STO(001). The signal at the $(00\frac{1}{2})$ position of the specular CTR is modulated by roughness fringes (R) with a periodicity of 1 ML and Kiessig fringes (K) every 2 MLs.

FIG. 2. Evolution of the $(0\,0\,\frac{1}{2})$ specular x-ray signal during the deposition of 1 ML of LSMO on STO, using 17 12-laser shot bursts, separated from one another by several seconds to allow the atoms to thermally diffuse to their optimal sites and minimize the atomic roughness. The change in x-ray reflectivity in between laser bursts was fit using Eq. (1) and is shown by the solid black curves. The inset shows the time constants for these fits. A linear regression fit of the dependence of τ_2 on θ is also shown (straight solid line).

smaller sized islands, which are hence separated from one another approximately by a distance equal to the unit-cell size multiplied by the square root of the number of shots required to deposit a single ML (here $\sqrt{200} \approx 14$), i.e., 5 to 6 nm. This simple model does not consider the strongly ionic nature of the deposited material—the chemical potential to spontaneously produce ordered unit cells for these ionic materials is high and will assist adatoms to diffuse to optimal sites.

The diffusion constant τ_2 is predicted by Eq. (2) to increase linearly from the start of ML growth. A linear regression of the data in the inset of Fig. 2 shows, however, that τ_2 becomes nonzero only after $\theta \approx 0.55$. Although at very low coverages, hyperthermal surface diffusion on the picosecond time scale, induced by the impinging species, can also enhance the nucleation of the stable nucleation sites, prior to this critical coverage no significant thermal surface diffusion occurs across the top of the growing ML and the incident atoms are promptly inserted into the growing layer at the point of impingement. This can be explained as follows: The small island sizes imply that any atom impinging on top of them will be necessarily close to an island edge, allowing the prompt insertion mechanism for species having kinetic energies of the order of 10–20 eV. If the result is merely an increase in the lateral size of the island, however, this will enhance its resistance to any subsequent insertion events as lateral pushout of material becomes increasingly energetically unfavorable. Also, the probability of a particle impinging close to an island edge will become smaller as the islands spread laterally. However, theoretical studies for energetic Ag and Cu homoepitaxy have identified a second mechanism of island "breakup" or "chipping," which produces small daughter islands and suppresses the growth of large 2D islands [14,15]. Could this mechanism cause a similar island breakup in PLD of more strongly and directionally bonded ionic oxide systems?

To answer this, we consider three surface configurations which may be typical: (i) atoms embedded in the surface layer far from an island edge; (ii) five atoms (La/Sr, Mn, and 3 O atoms) making up a surface unit cell [Fig. 3(a)]; (iii) ten atoms consisting of two such unit cells in a line [Fig. 3(b)]. We take tabulated bond strengths of La-O, Sr-O, and Mn-O of 800, 430, and 400 kJ mol^{-1} [21], and make the simplification of ignoring changes in individual dangling-bond energies. Surface La/Sr and Mn atoms not at island edges [i.e., case (i)] are eightfold and fivefold coordinated, respectively; hence transfer of kinetic energy to breaking bonds in excess of 20, 25, and 65 eV is required for sputtering of Mn, Sr, and La, respectively [22]. This will be most efficient if the impinging atom has the same mass as the struck surface atom. Typical kinetic energies for ablation species in PLD lie in the range of 5 to 25 eV [2]. Therefore disruption of surface atoms not at an island edge appears to be inefficient.

An isolated surface unit cell of La$_{1-x}$Sr$_x$MnO$_3$ [case (ii)] contains 3 La/Sr-O and 3 Mn-O bonds (not counting those
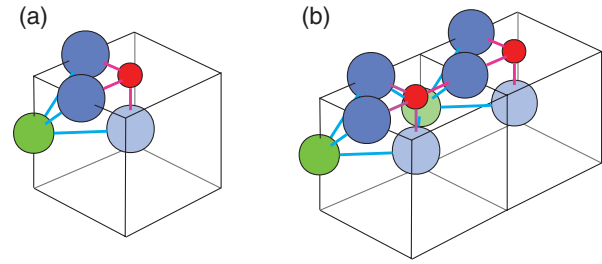

FIG. 3 (color). The positions and bonds of (a) a single unit-cell island and (b) a double unit-cell island. La/Sr, green; Mn, red; O, blue; La/Sr-O bond, cyan; Mn-O bond, magenta.

connecting the unit cell perpendicularly to the substrate), while an island consisting of two unit cells [i.e., case (iii)] contains 8 La/Sr-O and 7 Mn-O bonds. The difference in bonding energy between a double unit-cell island and 2 single unit-cell islands is therefore ≈ 16 eV, well within the typical energy range of the impinging species. The activation barrier between these two configurations is more difficult to estimate, but is likely to be reduced by electron-phonon coupling on the picosecond time scale [23].

Assuming the validity of the island breakup mechanism, the density of small islands will increase until they begin to coalesce, which will occur when the distance between them is approximately the same as their size, i.e., at $\theta = 0.5$ [19], which indeed we observe. Prior to this, there is negligible τ_2 diffusion; hence, Eq. (2) is modified to

$$\tau_2 = \frac{\theta - \theta_{\min}}{D_S(\mu_l^{(0)})^2 \pi N_S}, \qquad (3)$$

where $\theta_{\min}$ is the minimum coverage, below which mass transfer from on top of the growing layer to the growing layer is via prompt insertion. After this minimum coverage is reached, nonthermal smoothing in conventional PLD continues not only because the impinging particles have a transiently enhanced surface diffusion, but also because their transferred energy couples to those adatoms on the surface which have yet to find a stable site. This model appears to be particularly strong compared to other known competing nonthermal mechanisms (such as resputtering, enhanced surface diffusion alone, or implantation) as it is the only one that would show the sudden change in relaxation behavior at $\approx 50\%$ ML coverage, due to the fact it is the only one that depends on the microscopic morphology (i.e., the islands' size and surface density).

Therefore, for the first half of ML coverage, nucleation and island breakup at or near the point of impingement dominate. The average distance for adatoms *thermally* diffusing in the growing ML to ascending island edges (which determines τ_1) is for low θ comparable to the enhanced diffusion length and thereafter becomes smaller, which explains why τ_1 is so much shorter than τ_2. The processes leading to 2D monolayer growth in this model are summarized schematically in Fig. 4.

We can estimate the effective increase in surface temperature induced by PLD from a comparison of times to
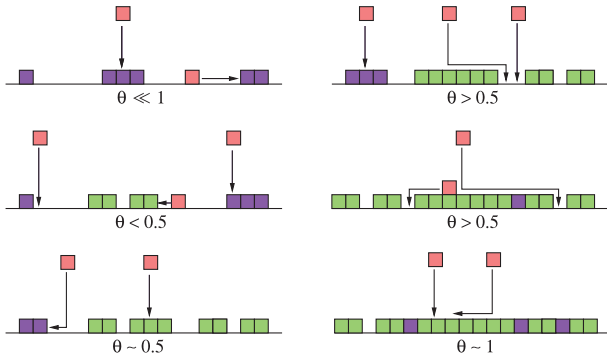
FIG. 4 (color). Summary of the proposed processes influencing long-term 2D film growth by PLD. At low coverage, the impinging particles (red) nucleate small, relatively densely packed islands (blue). Any impinging particles landing on top of these islands can cause them to split into daughter islands (green). The density of the small islands subsequently increases, such that at ≈ 50% coverage, their separation is approximately equal to their size, and the islands begin to coalesce, excluding further breakup. After this, the impinging species must diffuse to descending edge steps, which is accelerated by the energy of the impinging particles now coupling to diffusing adatoms.

produce atomically flat layers in conventional PLD and the characteristic thermal diffusion times between laser bursts in interrupted PLD. If we assume that typical surface diffusion constants for metal oxides lie between $D_0 = 10^{-4} \rightarrow 10^{-8}$ cm^2 s^{-1}, and that, toward ML completion, the adatoms have to travel between $\rho = 4$ and 25 nm to find a stable site, we obtain from the thermal diffusion data in the inset of Fig. 2 and a growth temperature of 1000 K a value of E_a that ranges between 2.2 eV ($D_0 = 10^{-4}$ cm^2 s^{-1}, $\rho = 4$ nm) and 1.1 eV ($D_0 = 10^{-8}$ cm^2 s^{-1}, $\rho = 25$ nm). We have seen in conventional PLD that enhancement of surface diffusion enables all the adatoms to find stable sites within the 0.1 s in between laser shots, even at high coverage. Using our values for E_a, we obtain an effective increase in the surface temperature of between 370 K ($D_0 = 10^{-4}$ cm^2 s^{-1}, $\rho = 4$ nm) and 1200 K ($D_0 = 10^{-8}$ cm^2 s^{-1}, $\rho = 25$ nm). These represent the limits. "Typical" estimates of $D_0 = 10^{-6}$ cm^2 and $\rho = 8$ nm yield $\Delta T \approx 500$ K.

In conclusion, prompt insertion of impinging ablation species into small-diameter 2D islands causing them to break up into daughter islands is proposed to explain the kinetics of long-term 2D thin film growth of complex metal-oxides using PLD. This mechanism restricts the lateral size of the islands up to a coverage of about 50%, at which point they begin to coalesce, shutting off the breakup mechanism. Thereafter, the kinetic energy of the impinging species is channeled into enhanced surface diffusion of the adatoms, which yields an effective increase in temperature (at least with respect to the degrees of freedom of lateral surface movement) of the order of 500 K. In this manner, monolayer completion is sufficiently efficient to allow 2D growth up to several tens of nm thickness. The authors believe such behavior has been recorded but not

recognized elsewhere [8], and that a judicious tuning of the energies of the incident species (which can be brought about by adjusting the laser fluence and/or the degree of quenching by a background moderating gas) could lead to this becoming a general phenomenon for a large range of chemical systems. Finally, theoretical models of multielemental thin film growth far from thermal equilibrium can now be verified against these unique quantitative experimental results.

*Electronic address: philip.willmott@psi.ch
[1] M. B. Salamon and M. Jaime, Rev. Mod. Phys. **73**, 583 (2001).
[2] P. R. Willmott and J. R. Huber, Rev. Mod. Phys. **72**, 315 (2000).
[3] P. R. Willmott, Prog. Surf. Sci. **76**, 163 (2004).
[4] G. K. Hubler and J. A. Sprague, Surf. Coat. Technol. **81**, 29 (1996).
[5] M. E. Taylor and H. A. Atwater, Appl. Surf. Sci. **127–129**, 159 (1998).
[6] R. M. Tromp and J. B. Hannon, Surf. Rev. Lett. **9**, 1565 (2002).
[7] H. Jenniches, M. Klaua, H. Höche, and J. Kirschner, Appl. Phys. Lett. **69**, 3339 (1996).
[8] G. Rijnders, G. Koster, V. Leca, D. H. A. Blank, and H. Rogalla, Appl. Surf. Sci. **168**, 223 (2000).
[9] J. M. Warrender and M. J. Aziz, Appl. Phys. A **79**, 713 (2004).
[10] B. Shin, J. P. Leonard, J. W. McCamy, and M. J. Aziz, Appl. Phys. Lett. **87**, 181916 (2005).
[11] A. Fleet, D. Dale, Y. Suzuki, and J. D. Brock, Phys. Rev. Lett. **94**, 036102 (2005).
[12] S. Stoyanov and M. Michailov, Surf. Sci. **202**, 109 (1988).
[13] M. Villarba and H. Jónsson, Surf. Sci. **324**, 35 (1995).
[14] J. Jacobsen, B. H. Cooper, and J. P. Sethna, Phys. Rev. B **58**, 15 847 (1998).
[15] J. M. Pomeroy, J. Jacobsen, C. C. Hill, B. H. Cooper, and J. P. Sethna, Phys. Rev. B **66**, 235412 (2002).
[16] B. D. Patterson *et al.*, Nucl. Instrum. Methods Phys. Res., Sect. A **540**, 42 (2005).
[17] P. R. Willmott, R. Herger, M. C. Falub, L. Patthey, M. Döbeli, C. V. Falub, M. Shi, and M. Schneider, Appl. Phys. A **79**, 1199 (2004).
[18] P. R. Willmott *et al.*, Appl. Surf. Sci. **247**, 188 (2005).
[19] A. J. H. M. Rijnders, Ph.D. thesis, University of Twente, 2001.
[20] T. Diaz de la Rubia, R. S. Averbach, R. Benedek, and W. E. King, Phys. Rev. Lett. **59**, 1930 (1987).
[21] *Handbook of Chemistry and Physics*, edited by D. R. Lide (CRC Press, Boca Raton, 1993).
[22] D. K. Brice, J. Y. Tsao, and S. T. Picraux, Nucl. Instrum. Methods Phys. Res., Sect. B **44**, 68 (1989).
[23] R. J. Hamers, Surf. Sci. **583**, 1 (2005).